Supramolecular Assembly of End-Functionalized Polymer Mixtures Confined in Nanospheres

June Huh,[‡] Ji Young Jung,[†] Jea Uk Lee,[†] Heesook Cho,[§] Soojin Park,[§] Cheolmin Park,[‡] and Won Ho Jo*,[†]

[†]Department of Materials Science and Engineering, Seoul National University, Seoul 151-742, Korea, [‡]Department of Materials Science and Engineering, Yonsei University, Seoul, Korea, and [§]Interdisciplinary School of Green Energy, Ulsan National Institute of Science and Technology, Ulsan, Korea

ABSTRACT Supramolecular assembly of functionalized polymers, capable of forming block copolymer-like molecular clusters, has emerged as a promising alternative for creating nanoscopically ordered structures. Here, we demonstrate that nanospheres, which have intriguing internal nanodomains and controllable surface functionality, can be fabricated by supramolecular assembly of two complementarily end-interacting species of mono-end-functionalized polymers using the self-organized precipitation (SORP) method. An exotic internal morphology, hierarchically organized structure of perforated spherical layers, was formed inside the nanosphere prepared from the stoichiometric mixture of the end-functionalized polymers, which is due to the formation of diblock-like supramolecules and their packing frustration in the spherically confined nanospace. When the mixing ratio of the two end-functionalized polymers differs from the stoichiometric ratio, the nanoparticle surface is enriched with an excess of unpaired functionalized groups, which therefore provides us with a useful way to precisely control the surface functionality of the nanoparticles.

KEYWORDS: end-functionalized polymers · phase separation · confined morphology · nanoparticles · supramolecular assembly

Specific interactions between molecules or molecular subgroups play an essential role in many self-assembling systems that show unique structural order inside the resultant molecular clusters. Those interactions include hydrogen bonding,[1−4] ionic interactions,[5−7] charge-transfer complexation,[8] coordination complexation,[9] and so on.[10,11] In the polymer blend systems where the constituent polymers are macroscopically phase-separated due to ubiquitous repelling interactions between dissimilar monomer species, the introduction of small functional groups capable of specific interactions can lead to an interesting self-assembly behavior that cannot be observed in the neat polymer blends. One of the simple examples is the binary blend of mono-end-functionalized polymers, viz., A-*x*/B-*y*, where the specifically attractive interactions between the end-functional pair *x* and *y* compete for mixing or demixing with the repulsive nonspecific interactions between polymers A and B. The frustration caused by these two opposing interactions is relieved in the best way by the formation of molecular clusters resembling chemically linked block copolymers, which leads the polymer blend to be nanoscopically phase-separated while at the same time maximizing the number of specific interactions between *x* and *y*. Previous experimental[3,9,12−15] and theoretical[16−22] works including ours have demonstrated that the physically end-linked AB cluster as a supramolecular analogue of an AB block copolymer has all the richness of morphological behaviors that block copolymers can exhibit, displaying distinctive crystal-like nanostructures and ordering transitions in the molten state. However, while this supramolecular concept using functionalized polymers has turned out to be a very promising alternative for developing nanoscopically ordered structures, very few works have tested this concept in combination with various processing variables such as solvent treatment, mechanical fields, electric fields, and spatial confinement entailing surface fields. In particular, the supramolecular assembly of functionalized polymer mixtures under confined geometry has never been reported before. Applying such processing methods is now becoming conventional in the current block copolymer nanotechnology for tailoring nanostructures suitable for specific applications.[23−26] Thus, the understanding of supramolecular assembly of functionalized polymers under various processing conditions is unquestionably essential for developing a technology toward the well-designed fabrication of supramolecular nanostructures.

Self-assembly of polymers within nanospace has attracted growing interest as a

*Address correspondence to whjpoly@ snu.ac.kr.
Phone: +82-2-880-7192.
Fax: +82-2-876-6086.

Received for review July 28, 2010 and accepted November 24, 2010.

Published online December 3, 2010.
10.1021/nn101805z

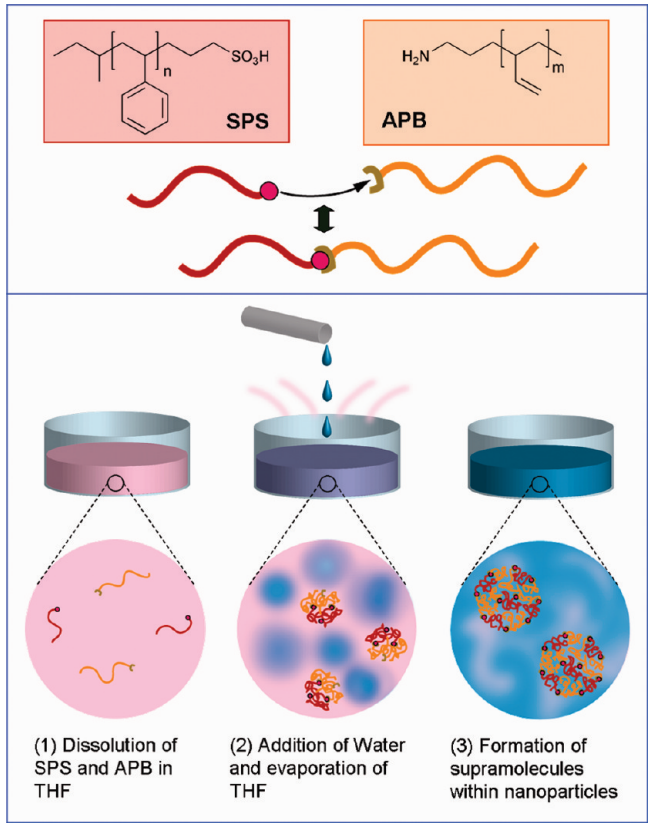

Figure 1. Schematic representation of the procedure of nanoparticle formation from a mixture of mono-end-sulfonated polystyrene and mono-end-aminated poly(1,2-butadiene).

means for miniaturization of structural objects or creating novel nanostructures, partly stimulated by the recent development in the production of polymer nanoparticles. As a notable method for manufacturing polymer nanoparticles, the self-organized precipitation (SORP) method provides an easy and robust route that can be applied to various polymers ranging from homopolymers to copolymers.[27−32] This method is based on the polymer precipitation in solvent where the solvent quality for a solute polymer is slowly changed from good to poor, achieved by the addition of droplets of a nonvolatile, poor solvent to the polymer dissolved in a volatile, good solvent. Here, on the basis of the SORP and the supramolecular assembly of a mono-end-functionalized polymer mixture, A-*x*/B-*y*, we report the fabrication of nanospheres that themselves have intriguing internal nanodomains of multilevel perforated spheres that have high specific interfacial area. The surface functionality of fabricated nanospheres can also be controlled by varying the mixing ratio of two types of end-functionalized polymers, which therefore enables us to tailor the surface activity of the nanospheres.

RESULTS AND DISCUSSION

Nanoparticle Preparation. Our method for preparing nanospheres is based on the SORP of mono-end-sulfonated polystyrene (SPS) and mono-end-aminated poly(1,2-butadiene) (APB) at room temperature. As schematically depicted in Figure 1, a mixed solute consisting of SPS (M_n = 10.5 kg/mol, polydispersity index = 1.05) and APB (M_n = 15.0 kg/mol, polydispersity index = 1.05) with a weight fraction of SPS (Φ) is first dissolved in tetrahydrofuran (THF), chosen as a good solvent for both polymers. Subsequently, water drops are slowly added to the end-functionalized polymer solution, which provides a driving force for the polymers to form temporal aggregates near each water droplet. The formation of these fluctuating, temporal aggregates becomes stabilized more and more by the steady addition of water droplets and the simultaneous evaporation of volatile THF. While the added water gradually becomes a majority solvent, the minority THF solvent, miscible with both polymers and water, plays a role similar to a colloidal stabilizer, preventing polymer aggregates from excessive growth. During this gradual change of solvent quality leading to the polymer assembly to nanospheres, the 1:1 end-associations between SPS and APB chains occur due to strong ionic interaction between a proton-donating sulfonic acid group of SPS and a proton-accepting amino group of APB ($SO_3^- \cdots NH_3^+$), which determines the morphological structure within the nanoparticle in combination with other interactions including the nonspecific repulsion between styrene and butadiene segments. It should also be mentioned that the end-association between SPS and APB may be interrupted by the presence of water molecules capable of forming hydrogen bondings with sulfonic acid groups during the SORP process. However, considering that the amino group is a much stronger proton acceptor than a water molecule,[33] and that both SPS and APB are insoluble in water to form coaggregates, it is conjectured that the end-associations of sulfonic acid groups with amino groups are predominant within the polymer aggregates.

Internal and Surface Morphology. The SPS weight fraction in the mixed solute, Φ, is the primary variable for controlling the structure of nanospheres in this study. We begin with the case of a stoichiometric mixture ($\Phi = \Phi_{ST}$) where the number of sulfonic acid groups of SPS chains is equal to the number of amino groups of APB chains. The transmission electron microscopy (TEM) images of the nanoparticles prepared from a mixed solute of SPS and APB with Φ = 0.40 ($\cong \Phi_{ST}$) and their cryotomed section are shown in Figure 2a and b, respectively, where the darker phase corresponds to the APB domains stained by osmium tetraoxide (OsO_4) and the lighter phase to SPS domains. The images show a very interesting internal morphology that appears at first glance to be concentric dashed circles of SPS domains embedded in the majority APB phase. It is worth noting that the internal morphology shown in Figure 2a and b is completely different from the confined binary polymer blends without end-functionalization.[30,34] An experimental study of SORP of polystyrene (PS)/polyisoprene (PI) blends in THF/water, which is very

similar to the present system apart from end-functionalization, has reported a Janus-like internal morphology where PS and PI are phase-separated into two hemispherical domains.[30] This suggests that the end-functionality plays a significant role in the structure formation inside the particles. It is also confirmed that the dispersion of nanoparticles and their internal structures are unchanged even after prolonged standing of vials containing nanoparticle dispersion (more than 5 months).

To figure out the three-dimenisonal geometry of this exotic internal morphology, we simulated a model system using density functional theory under an assumption that all the SPS and APB chains are end-linked to form styrene−butadiene (SB) diblock-like supramolecules. For the simulation, we numerically integrate the Cahn−Hilliard−Cook (CHC) diffusion equation with the Landau−Ginzburg (LG) free energy[35−40] and a surface field in a spherical volume, where both the conformational contributions of the SB diblock and the pairwise interactions between the components (i.e., styrene (S), butadiene (B), and water (W)) are taken into account.[41−43] Figure 2c−e represents the simulated morphologies of the model nanosphere, showing its surface and internal morphologies. The simulated morphologies reveal that the dashed circle-like SPS domains shown in Figure 2b are actually spherical layers perforated by several APB struts connecting concentric APB layers at different levels. The structural hierarchy of the perforated spheres in a fashion of spheres-in-sphere is shown in more detail in Figure 2e, which clearly shows the mesh-like SPS spherical layers at each level. It is noteworthy that the stoichiometric mixture of strongly associating SPS and APB would form a gyroid phase in the bulk state at room temperature, although an experimental confirmation for the molten bulk morphology of a stoichiometric mixture of SPS and APB at room temperature is not possible due to the glass transition temperature of SPS (~95 °C), higher than room temperature. Nevertheless, when the bulk morphology of the mixture is investigated at 110 °C instead of room-temperature conditions, it is observed from the TEM image that the bulk morphology appeared to be a gyroid phase (Supporting Information, Figure S1). Since the decrease of temperature from 110 °C to room temperature corresponds to the increase in $N\chi$ from $N\chi \cong 16$ to $N\chi \cong 22$,[44] the bulk structure of the stoichiometric SPS/APB mixture at room temperature, which behaves like a polystyrene−polybutadiene (PS-PB) diblock copolymer with a 40 wt % styrene content (36 vol.%) in the intermediate segregation regime, seems to be still within the region of gyroid phase when inferred from the theoretical phase diagram of the diblock copolymer.[45] It is known that the gyroid phase is highly competitive with the perforated layer (PL) in the composition range 32−44 vol %, although the PL phase turns out to be only metastable in bulk conditions.[46] As one can conceive, the geometric misfit between spherical confinement and the gyroidal unit cell is responsible for the formation of the perforated sphere that is a version of the PL phase conforming to the spherical geometry. Under tight spherical confinement, the accommodation of a gyroidal unit cell would impose high stress on the system. Similar morphological modulation has been observed in the case of a spherically confined PS-PB diblock copolymer.[47]

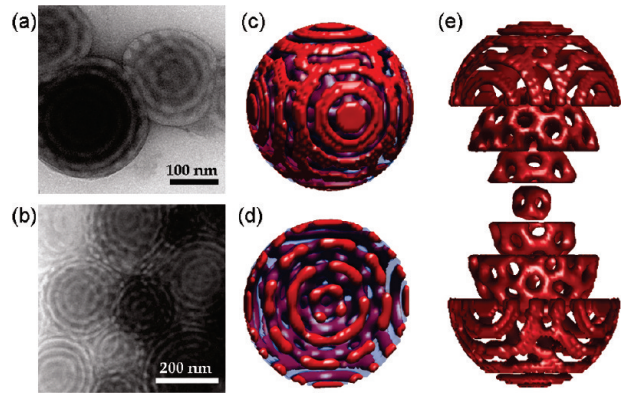

Figure 2. Nanoparticles prepared from a mixed solute of SPS and APB with $\Phi = \Phi_{ST}$. (a) TEM image of the produced nanoparticles and (b) TEM image of cryo-sectioned nanoparticles. (c) Simulated nanosphere and (d) its internal structure represented by a radial cross section. Regions of high density of SPS and APB are colored opaque red and transparent blue, respectively. (e) The decomposed representation of hierarchical perforated spheres.

We have just shown that the nanoparticle prepared from the stoichiometric mixture of SPS and APB has a hierarchically ordered internal structure of perforated spheres owing to the formation of diblock-like supramolecules and their packing frustration in the nanosphere. The strong tendency of sulfonic acid groups associating with an amino group rather than with water molecules can also be inferred from the fact that SPS and APB domains are regularly spaced from each other even at the surface of nanoparticles, as seen in Figure 2a and b, although the particle surface is exposed to water solvent.

It is interesting to examine how the surface and internal morphology of nanoparticles are altered when the SPS/APB mixture becomes nonstoichiometric with an excess of SPS chains that may form hydrogen bondings with water molecules. Figure 3 compares the morphologies of nanoparticle samples prepared from SPS/APB mixtures with $\Phi = 0.40$, $\Phi = 0.45$, $\Phi = 0.50$, and $\Phi = 0.70$. It is observed that the perforated spheres, similar to the structure of the stoichiometric case, are formed inside a uniform outermost SPS layer for $\Phi = 0.45$ (Figure 3b) and $\Phi = 0.50$ (Figure 3c). As the SPS fraction is increased further to $\Phi = 0.70$, the inner morphology becomes a uniformly layered structure where SPS and APB form concentric domains (Figure 3d). Similar morphological transformation from PL to lamellar phase has been reported for a cylindrically confined gyroid-forming block copolymer system.[48] It should also

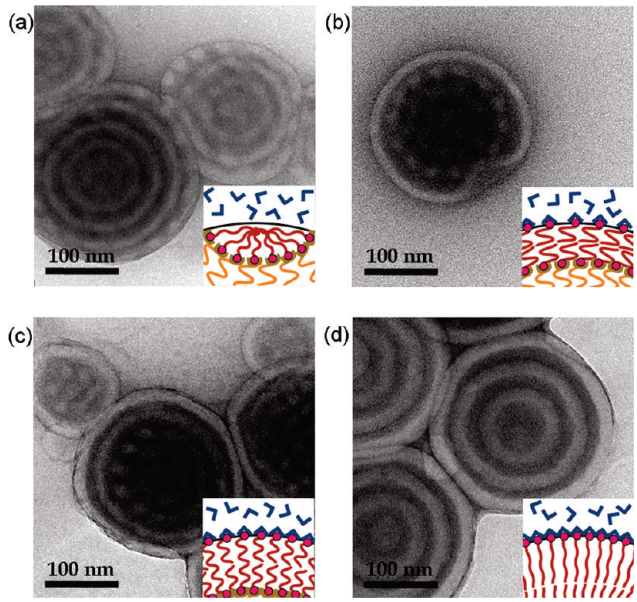

Figure 3. TEM images of internal morphologies of nanoparticles from a mixed solute of SPS and APB with (a) $\Phi = 0.4$, (b) $\Phi = 0.45$, (c) $\Phi = 0.5$, and (d) $\Phi = 0.7$. The schematics in the insets represent the molecular arrangements near the surface of the nanoparticles.

be noted from Figure 3d that the thickness of the SPS outermost layer (~20 nm) is the same as the thicknesses of SPS layers in the interior region (~20 nm). This clearly differs from the case of a confined block copolymer, where the outermost layer is always half the thickness of the inner domains.[49]

It is noted that the outermost SPS layer becomes thicker as Φ increases from Φ_{ST}, indicating that the outermost layer is enriched with SPS chains possibly due to the formation of hydrogen bondings between excessive sulfonic acid groups and water molecules. The process of this surface enrichment of SPS chains by increasing Φ can be interpreted by the following. At $\Phi = \Phi_{ST}$, most of the sulfonic acid end-groups of the SPS chains are associated with the amino end-groups of APB chains to form diblock-like supramolecules, and only very small portion of them are exposed to the water solvent. On the other hand, when $\Phi > \Phi_{ST}$, the excess SPS chains form the outermost layer as they form SPS brushes stretching inward from the surface at which the sulfonic acid end-groups are hydrogen-bonded with water molecules. Therefore, as shown in the schematics of Figure 3b−d, the SPS chains paired with water molecules and with APB chains form a bilayer in the outermost SPS domain, and the bilayer becomes thicker as Φ increases to stretch inward away from the surface of the nanosphere due to volume conservation. With this speculation, we can estimate the number of water-exposed (or hydrogen-bonded) sulfonic acid groups per unit of surface area (σ), assuming that all the APB chains are end-linked with SPS chains and that the nanosphere surface is enriched only with excess SPS chains. By a simple geometric argument, the area density σ is given as $\sigma = \rho_o D(\varphi - \varphi_{ST})/[6N_{SPS}(1 - \varphi_{ST})]$, where N_{SPS} is the degree of polymerization of SPS, ρ_o is the average monomer density in the SPS/APB mixture, D is the diameter of the nanosphere, and φ and φ_{ST} are the volume fraction and the stoichiometric volume fraction of SPS in the mixed solute, respectively. The formula suggests that σ is linear to φ provided that the diameter of the nanosphere, D, is independent of φ. Indeed, it is confirmed from the dynamic light scattering (DLS) measurement that the average diameter of the nanoparticle is nearly independent of the SPS fraction, being in the range 260−280 nm (Supporting Information, Figure S2). Using the parameters that $N_{SPS} \cong 100$, $\rho_o \cong 7.6\ nm^{-3}$, and $D \cong 270$ nm,[44] we obtain $\sigma \cong 0.21$, 0.48, and 1.59 nm^{-2} for the three cases of $\Phi = 0.45$, 0.50, and 0.70 ($\varphi = 0.41$, 0.46, and 0.66), respectively. A large value of σ, which should be accompanied with the stretching of SPS chains in the outermost layer due to volume conservation, leads to the reduction in the overall SPS/APB interfacial area inside the nanoparticle. Conversely, the energetic propensity of decreasing the overall SPS/APB interfacial area also contributes to an increase in σ, which compromises an entropic penalty associated with stretching of SPS chains in the outermost layer. It should also be noted that the estimation of σ is based on the assumption that all the excess SPS chains contribute to form the outmost brush layer. However, there is certainly a limiting value for σ (typically ~1 nm^{-2}) as the chains become highly stretched in the brush layer (see the schematic in Figure 3d). When the outermost SPS brush layer cannot accommodate SPS chains any more, the rest of the excess SPS chains may enter the SPS domains in the interior region of the nanosphere, which gives rise to a phase transformation of internal morphology at $\Phi \gg \Phi_{ST}$. This may happen in the case of $\Phi = 0.70$, at which the uniform spherical layers are formed instead of perforated spheres, as shown in Figure 3d.

Surface Functionality. As discussed above, the surface and the inner morphologies of nanoparticles suggest that the produced nanoparticles have surface functionalities of sulfonic acid groups due to the surface enrichment of excess SPS chains. In order to directly identify the surface functionality of the produced nanoparticles, a fluorescent pyrene derivative, 1,6-diaminopyrene (DAPY), was used to probe the surface of the nanoparticles. The probe molecule DAPY can be physisorbed onto the surface of the nanoparticles *via* specific interactions between the exposed SO_3H groups of SPS and NH_2 groups of DAPY, which therefore allows us to optically detect the sulfonic acid groups exposed on the nanoparticle surface by measuring fluorescence emission. To do this, the solution of DAPYs in methanol was added to the nanoparticle dispersions prepared by the SORP method described previously. The nanoparticle dispersions containing DAPYs were then dialyzed against methanol using a porous membrane to remove DAPYs unadsorbed to the nanoparticle surface.

Figure 4a presents the fluorescence (FL) emission spectra of the nanoparticle dispersions with DAPYs excited at 334 nm for $\Phi = 0.4$, 0.5, 0.6, and 0.7. Since a significant excimer emission ($\lambda_{em} = 442$) attributed to DAPY aggregations was not detected, it is considered that DAPYs are randomly physisorped on the surface of nanoparticles, as shown in the schematic of Figure 4b. The spectra show that the FL emissions at the wavelength $\lambda_{em} = 377$ nm and $\lambda_{em} = 397$ nm, both arising from the nonaggregated DAPY molecules, concurrently increase as Φ increases, indicating that the number of sulfonic acid groups at the nanosphere surface increases with increasing weight fraction of SPS Φ. Furthermore, the linear relation between Φ and the FL intensity at $\lambda_{em} = 377$ nm (I_{377}) in the range $\Phi = 0.4-0.6$ and the deviation from the linearity at $\Phi = 0.7$ (inset in Figure 4a) support the aforementioned speculation about the surface enrichment of excess SPS and the internal morphology transformation from perforated sphere to uniformly layered structure. The specific interaction of DAPY amino groups with sulfonic acid groups rich on the surface of the nanoparticle in the case of $\Phi = 0.7$ is further evidenced by confocal images, as shown in Figure 4c, where the spots of blue fluorescence are exactly positioned at each individual nanoparticle or the nanoparticle aggregates formed by DAPYs bridging between nanoparticles.

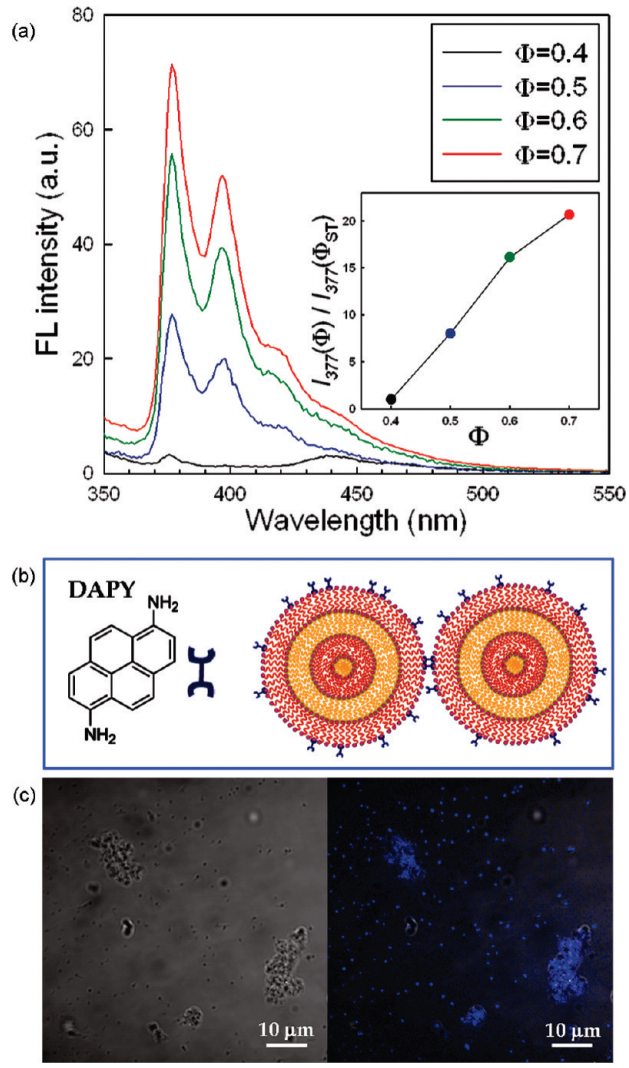

Figure 4. (a) FL emission spectra of nanoparticle dispersions with DAPYs for $\Phi = 0.4$, $\Phi = 0.5$, $\Phi = 0.6$, and $\Phi = 0.7$. The inset shows the normalized FL intensity at $\lambda_{em} = 377$ nm with respect to the intensity of $\Phi = 0.4$ as a function of Φ. (b) The schematic representation of the physisorption of DAPY onto the nanoparticle surface *via* specific interaction between the NH_2 group of DAPY and the SO_3H group of SPS. (c) The confocal images of DAPY-physisorbed nanoparticles for $\Phi = 0.7$.

Other Effects. While the SPS fraction in the mixture solute is a key parameter to control the surface functionality of the nanoparticles, it is also important to find out processing variables for controlling the size of the nanoparticles. Figure 5 presents the diameter of the nanoparticles ($\Phi = 0.70$) plotted against the overall concentration of polymers (Figure 5a) and against the ratio of the volume of added water to the initial volume of THF solvent (Figure 5b). It is found that the diameter increases linearly with the polymer concentration in the investigated concentration range (0.1−0.5 g/L), whereas it is nearly independent of the volume ratio of water to THF, although it shows a slight decrease as the water/THF volume ratio increases. It is worth mentioning that the latter dependence is much weaker than the dependence reported for the SORP of polymers consisting only of hydrophobic monomers.[27] The difference is possibly attributed to the colloidal nature of the nanoparticles in the present case where rich surface functionality does not sensitively care about the volume ratio between water and THF. It is also confirmed that the size of the produced particles is nearly insensitive to the stirring conditions accessible in the experiment when judging from the opaqueness of particle dispersions.

Lastly, we discuss some factors affecting the end-association in the SORP process. As reported in our previous theoretical studies on the blend of end-functionalized polymers,[19] the degree of end-association is governed by a ratio $\kappa = f_o/(N\chi k_BT)$, characterizing the competition between the magnitude of end-association interaction, f_o, and the degree of incomaptibity, $N\chi$. For the case where end-association is strong enough to produce block copolymer-like supramolecule, the ratio κ should be larger than a critical value, κ_c ($\sim O(1)$) so that proper choices for functional pair (f_o), polymer pair (χ), and the degree of polymerization (N) of the constituent polymers are necessitated. While the present system of SPS/APB in THF/water seems to be a system satisfying this criterion ($\kappa > \kappa_c$), any changes disobeying the criterion would result in macroscopic phase separation instead of the formation of an ordered structure. Indeed, when mono-end-carboxylated polystyrene (CPS), which has nearly the same molecular weight (10 kg/mol) as that of SPS, is used as a partner polymer for APB in the SORP process,

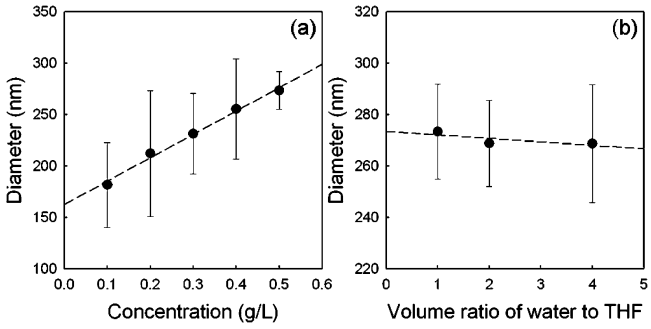

Figure 5. The diameter of the nanoparticles prepared from the SPS/APB mixture with $\Phi = 0.7$ as a function of (a) polymer concentration and (b) volume ratio water to THF.

it is found that the nanoparticles from CPS/APB are also well-produced, but their internal morphology shows indefinite shape and organization of CPS and APB domains (Supporting Information, Figure S3) possibly due to the weaker protic nature of the carboxylic acid group of CPS than the sulfonic acid group of SPS. Similar weakening of end-association is found when the solvent pair THF/water is replaced by THF/acetic acid in the SORP of SPS/APB, which leads to a poorly ordered internal structure since the end-association is more interrupted by acetic acid than water (Supporting Information, Figure S4).

SUMMARY

Nanospheres comprised of two complementarily end-interacting species of polymers have been fabricated by the SORP method. An exotic internal morphology, hierarchically organized perforated spheres, was formed inside the nanosphere prepared from the stoichiometric mixture, resulting from the formation of diblock-like supramolecules and their packing frustration in the spherically confined nanospace. The thickening of the outermost brush layer, accompanied by the enrichment of functionalized groups on the nanoparticle surface, was observed by changing the mixing ratio of the two end-functionalized polymers, which allows us to precisely control the surface functionality of the nanoparticles. The suggested mechanism for this disciplined molecular organization of end-functionalized polymers in solvent media provides a guideline to tune both the surface functionality and the internal morphology of nanoparticle, which can be essential for further physical or chemical decoration needed in various applications. A specific application would be a particulate substance having high functionality that rapidly provides *ex vivo* medical diagnostic tests where the rapidness and sensitivity of the diagnosis is highly required. The richness of functionality can be even more intensified by cross-linking one of the components (e.g., APB) followed by removing the un-cross-linked component to expose functionalities at the interface in the interior region of the nanoparticles. The multilevel perforated structure, which has a large specific interfacial area, is particularly advantageous in that case.

METHODS

Preparation of Nanoparticle Dispersions. The polymer mixture of SPS and APB, purchased from Polymer Source Inc., was dissolved in THF to prepare a 0.5 g/L solution. Pure water (200 mL) was then added to the polymer mixture solution (100 mL) by a syringe pump with an injection rate of 1 mL/min under stirring. After the complete addition of water, THF was evaporated from the solution at room temperature for 2 days. For the preparation of nanoparticles onto which DAPY molecules are physisorbed, a solution of DAPY (Aldrich Inc.) in methanol (5 mL) was prepared at a concentration of 1 g/L and added to the nanoparticle dispersion (5 mL). The nanoparticle dispersions containing DAPYs were then dialyzed against methanol through a porous membrane for 3 days to remove unadsorbed DAPYs.

Measurement and Instruments. For TEM measurements of nanoparticles, drops of nanoparticle dispersion were put on a carbon-coated 300-mesh copper grid and dried at room temperature. The APB was preferentially stained by exposing to the vapor of osmium tetraoxide overnight. TEM images were taken in the bright-field mode using a JEOM 1010 (JEOL) operated at 80 kV accelerating voltages or using a JEM 2100 (JEOL) operated at 200 kV accelerating voltages. For cross-sectional TEM images, the nanoparticles embedded in concentrated sucrose were cryo-microtomed (RMC Ultracut) to a nominal thickness of ~80 nm at −120 °C and transferred to copper grids. The size of the nanoparticles was measured by an electrophoretic light-scattering spectrophotometer (ELS-8000, Otsuka Electronics) in the size measurement mode at a fixed angle of 90° at room temperature. The fluorescence emission spectra for nanoparticle dispersions with DAPYs were obtained from a fluorescence spectrometer (RF 5301, Shimadzu) by irradiating the dispersions at 334 nm. For imaging of the nanoparticle with DAPYs, the nanoparticle dispersion containing DAPYs was dropped onto a glass slide and localized by the addition of mounting medium (VECTASHIELD H-1000, Vector). Confocal images of nanoparticles were obtained using a confocal laser scanning microscope system with an upright confocal microscope (LSM510, Carl Zeiss) by irradiating the dispersions at 334 nm, where an LP filter of 377 nm was used for DAPY detection.

Computations. Assuming that all the SPS and APB chains in the stoichiometric mixture are end-linked to produce diblock copolymer-like supramolecules, the internal morphology of the mixture under spherical confinement is modeled as a spherically confined AB diblock copolymer melt that can be simulated in a spherical volume by Landau−Ginzburg approach on the basis of the Cahn−Hilliard−Cook (CHC) diffusion equation:[35−40]

$$\frac{\partial \psi(\mathbf{r})}{\partial t} = M\nabla^2\left(\frac{\partial (F + F_{surf})}{\partial \psi}\right) + \xi(\mathbf{r}) \qquad (1)$$

Here the order parameter ψ describes the deviation of the local A-monomer fraction from its average value at a position $\mathbf{r}$ (defined by $\psi(\mathbf{r}) = \varphi(\mathbf{r}) - \varphi$, where $\varphi(\mathbf{r})$ and φ are the local fraction of A-monomer and the mean fraction of A-monomer), M is a mobility constant set to unity, F is the free energy functional of the block copolymer, F_{surf} is the free energy associated with the interaction between the surface of confined geometry and the block copolymer, and ξ represents the thermal noise. The free energy functional, F, is given approximately by the Landau-type free energy:

$$F(\psi) \cong \int d\mathbf{r}\left[-\frac{\tau}{2}\psi^2(\mathbf{r}) + \frac{\mu}{3!}\psi^3(\mathbf{r}) + \frac{\lambda}{4!}\psi^4(\mathbf{r}) + \frac{D}{2}\{\nabla\psi(\mathbf{r})\}^2\right] + \frac{b}{2}\int d\mathbf{r}_1 \int d\mathbf{r}_2 G(\mathbf{r}_1 - \mathbf{r}_2)\psi(\mathbf{r}_1)\psi(\mathbf{r}_2) \quad (2)$$

Here τ is a temperature-like parameter related to the Flory interaction parameter between the A- and B-monomer (χ), and μ, λ, and D are related to the architecture of the block copolymer determining conformational contributions when the block copolymers are packed into a certain type of mesophase. The last term represents a long-range repulsion penalizing long-wavelength inhomogeneity through the Green function G with a period-controlling parameter b. The surface free energy, F_{surf}, is given as

$$F_{surf} = \int d\mathbf{r}\, s(\mathbf{r})\, \psi(\mathbf{r}) \quad (3)$$

where $s(\mathbf{r})$ is a surface field proportional to the difference in surface/polymer interfacial tension between surface/A and surface/B block and nonzero only at the position next to the spherical surface if the surface attracts one of the blocks ($s < 0$ if the surface is attractive to A-block and *vice versa*). The molecular parameters, τ, μ, λ, D, and b, for diblock architecture can be approximately given as

$$\tau = 2(\chi - \chi_s) + \frac{3^{1/2}}{N\varphi^{3/2}(1-\varphi)^{3/2}}, \mu = \Gamma_3/N, \lambda = \Gamma_4(0,0)/N, D = \frac{1}{12\varphi(1-\varphi)}, b = \frac{9}{N^2\varphi^2(1-\varphi)^2} \quad (4)$$

where χ_s is the χ at the spinodal, N is the number of statistical monomers of diblock copolymer, and Γ_3 and $\Gamma_4(0,0)$ are Leibler vertex functions computed from the monomer correlation functions.[41−43] The diffusion equation eq 1 is numerically integrated in the discrete space with the boundary condition for a spherical geometry of confinement.

The parameters used in the simulation are given by the following. The volume fraction, φ, of the minor component (i.e., SPS) in a spherical volume and the degree of incompatibity, χN, are set to be $\varphi = 0.36$ and $\chi N = 18$. The diameter of spherical volume, D, is given as the mean value of the produced nanospheres in the experiment: $D \cong 7L_o$ (~270 nm) where L_o is the bulk period of the diblock. The surface fields for the S/W and B/W interfaces are given by considering the surface tensions[50] of the S, B, and W components from which the S/W and B/W interfacial tensions are estimated using Fowkes' equation.[51]

Acknowledgment. This work was supported by a grant from the Fundamental R&D Program for Core Technology of Materials funded by the Ministry of Knowledge Economy, Republic of Korea. One of authors (J.H.) also acknowledges the support from the Korea Research Foundation through Grant KRF-2006-331-D00164.

Supporting Information Available: This material is available free of charge *via* the Internet at http://pubs.acs.org.

REFERENCES AND NOTES

1. Ruokolainen, J.; Mäkinen, R.; Torkkeli, M.; Mäkelä, T.; Serimaa, R.; ten Brinke, G.; Ikkala, O. Switching Supramolecular Polymeric Materials with Multiple Length Scales. *Science* **1998**, *280*, 557–560.
2. Tang, C.; Lennon, E. M.; Fredrickson, G. H.; Kramer, E. J.; Hawker, C. J. Evolution of Block Copolymer Lithography to Highly Ordered Square Arrays. *Science* **2008**, *322*, 429–432.
3. Feldman, K. E.; Kade, M. J.; de Greef, T. F. A.; Meijer, E. W.; Kramer, E. J.; Hawker, C. J. Polymers with Multiple Hydrogen-Bonded End Groups and Their Blends. *Macromolecules* **2008**, *41*, 4694–4700.
4. Sun, Z.; Bai, F.; Wu, H; Schmitt, S. K.; Boye, D. M.; Fan, H. Hydrogen-Bonding-Assisted Self-Assembly: Monodisperse Hollow Nanoparticles Made Easy. *J. Am. Chem. Soc.* **2009**, *131*, 13594–13595.
5. Shah, R. K.; Kim, J.-W.; Weitz, D. A. Janus Supraparticles by Induced Phase Separation of Nanoparticles in Droplets. *Adv. Mater.* **2009**, *21*, 1949–1953.
6. Bu, W.; Uchida, S.; Mizuno, N. Micelles and Vesicles Formed by Polyoxometalate-Block Copolymer Composites. *Angew. Chem., Int. Ed.* **2009**, *48*, 8281–8284.
7. Xiao, S.; Lu, X.; Lu, Q.; Su, B. Photosensitive Liquid-Crystalline Supramolecules Self-Assembled from Ionic Liquid Crystal and Polyelectrolyte for Laser-Induced Optical Anisotropy. *Macromolecules* **2008**, *41*, 3884–3892.
8. Wang, C.; Guo, Y.; Wang, Y.; Xu, H.; Wang, R.; Zhang, X. Supramolecular Amphiphiles Based on a Water-Soluble Charge-Transfer Complex: Fabrication of Ultralong Nanofibers with Tunable Straightness. *Angew. Chem.* **2009**, *121*, 9124–9127.
9. Lohmeijer, B. G. G.; Schubert, U. S. Supramolecular Engineering with Macromolecules: An Alternative Concept for Block Copolymers. *Angew. Chem., Int. Ed.* **2002**, *41*, 3825–3829.
10. Tan, L. H.; Xing, S.; Chen, T.; Chen, G.; Huang, X.; Zhang, H.; Chen, H. Fabrication of Polymer Nanocavities with Tailored Openings. *ACS Nano* **2009**, *3*, 3469–3474.
11. Weng, W.; Beck, B.; Jamieson, A. M.; Rowan, S. J. Understanding the Mechanism of Gelation and Stimuli-Responsive Nature of a Class of Metallo-Supramolecular Gels. *J. Am. Chem. Soc.* **2006**, *128*, 11663–11672.
12. Huh, J.; Park, H. J.; Kim, K. H.; Kim, K. H.; Park, C.; Jo, W. H. Giant Thermal Tunability of the Lamellar Spacing in Block-Copolymer-Like Supramolecules Formed from Binary-End-Functionalized Polymer Blends. *Adv. Mater.* **2006**, *18*, 624–629.
13. Binder, W. H.; Bernstoff, S.; Kluger, C.; Petraru, L.; Kunz, M. J. Tunable Materials from Hydrogen-Bonded Pseudo Block Copolymers. *Adv. Mater.* **2005**, *17*, 2824–2828.
14. Yang, X.; Hua, F.; Yamato, K.; Ruckenstein, E.; Gong, B.; Kim, W.; Ryu, C. Y. Supramolecular AB Diblock Copolymers. *Angew. Chem., Int. Ed.* **2004**, *43*, 6471–6474.
15. Pipas, S.; Floudas, G.; Pakula, T.; Lieser, G.; Sakellariou, S.; Hadjichristidis, N. Miktoarm Block Copolymer Formation *via* Ionic Interactions. *Macromolecules* **2003**, *36*, 759–763.
16. Tanaka, F.; Ishida, M.; Matsuyama, A. Theory of Microphase Formation in Reversibly Associating Block Copolymer Blends. *Macromolecules* **1991**, *24*, 5582–5589.
17. Huh, J.; ten Brinke, G. Micro- and Macrophase Separation in Blends of Reversibly Associating One-end-functionalized Polymers. *J. Chem. Phys.* **1998**, *109*, 789–797.
18. Angerman, H. J.; ten Brinke, G. Weak Segregation Theory of Microphase Separation in Associating Binary Homopolymer Blends. *Macromolecules* **1999**, *32*, 6813–6820.
19. Huh, J.; Jo, W. H. Theory on Phase Behavior of Triblock-like Supramolecules Formed from Reversibly Associating End-functionalized Polymer Blends. *Macromolecules* **2004**, *37*, 3037–3048.
20. Feng, E. H.; Lee, W. B.; Fredrickson, G. H. Supramolecular Diblock Copolymers: A Field-theoretic Model and Mean-field Solution. *Macromolecules* **2007**, *40*, 693–702.
21. Lee, W. B.; Elliott, R.; Katsov, K.; Fredrickson, G. H. Phase Morphologies in Reversibly Bonding Supramolecular Triblock Copolymer Blends. *Macromolecules* **2007**, *40*, 8445–8454.
22. Elliott, R.; Fredrickson, G. H. Supramolecular Assembly in Telechelic Polymer Blends. *J. Chem. Phys.* **2009**, *131*, 144906.
23. Park, S.; Lee, D. H.; Xu, J.; Kim, B.; Hong, S. W.; Jeong, U.; Xu, T.; Russell, T. P. Macroscopic 10-Terabit-per-Square-Inch Arrays from Block Copolymers with Lateral Order. *Science* **2009**, *323*, 1030–1033.
24. Thurn-Albrecht, T.; Schotter, J.; Kastle, C. A.; Emley, N.; Shibauchi, T.; Krusin-Elbaum, L.; Guarini, K.; Black, C. T.; Tuominen, M. T.; Russell, T. P. Ultrahigh-Density Nanowire Arrays Grown in Self-assembled Diblock Copolymer Templates. *Science* **2000**, *290*, 2126–2129.

25. Wu, Y. Y.; Livneh, T.; Zhang, Y. X.; Cheng, G. S.; Wang, J. F.; Tang, J.; Moskovits, M.; Stucky, G. D. Templated Synthesis of Highly Ordered Mesostructured Nanowires and Nanowire Arrays. *Nano Lett.* **2004**, *4*, 2337–2342.
26. Cheng, J. Y.; Mayes, A. M.; Ross, C. A. Nanostructure Engineering by Templated Self-assembly of Block Copolymers. *Nat. Mater.* **2004**, *3*, 823–828.
27. Yabu, H.; Higuchi, T.; Ijiro, K.; Shimomura, M. Spontaneous Formation of Polymer Nanoparticles by Good-solvent Evaporation As a Nonequilibrium Process. *Chaos* **2005**, *15*, 047505.
28. Yabu, H.; Higuchi, T.; Shimomura, M. Unique Phase-Separation Structures of Block-Copolymer Nanoparticles. *Adv. Mater.* **2005**, *17*, 2062–2065.
29. Higuchi, T.; Tajima, A.; Yabu, H.; Shimomura, M. Spontaneous Formation of Polymer Nanoparticles with Inner Micro-Phase Separation Structures. *Soft Matter* **2008**, *4*, 1302–1305.
30. Higuchi, T.; Tajima, A.; Motoyoshi, K.; Yabu, H.; Shimomura, M. Suprapolymer Structures from Nanostructured Polymer Particles. *Angew. Chem., Int. Ed.* **2009**, *48* (1−5), 31.
31. Motoyoshi, K.; Tajima, A.; Higuchi, T.; Yabu, H.; Shimomura, M. Static and Dynamic Control of Phase Separation Structures in Nanoparticles of Polymer Blends. *Soft Matter* **2005**, *127*, 5125–5131.
32. Hales, K.; Chen, Z.; Wooley, K. L.; Pochan, D. J. Nanoparticles with Tunable Internal Structure from Triblock Copolymers of PAA-b-PMA-b-PS. *Nano Lett.* **2008**, *8*, 2023–2026.
33. Gilli, P.; Pretto, L.; Bertolasi, V.; Gilli, G. Predicting Hydrogen-Bond Strengths from Acid-Base Molecular Properties. The pK(a) Slide Rule: Toward the Solution of a Long-Lasting Problem. *Acc. Chem. Res.* **2009**, *42*, 33–44.
34. Chen, D.; Chen, J.-T.; Glogowski, E.; Emrick, T.; Russell, T. P. Thin Film Instabilities in Blends under Cylindrical Confinement. *Macromol. Rapid Commun.* **2009**, *30*, 377–383.
35. Oono, Y.; Puri, S. Study of Phase-Separation Dynamics by Use of Cell Dynamical Systems. I. Modeling. *Phys. Rev. A* **1988**, *38*, 434–453.
36. Bahiana, M.; Oono, Y. Cell Dynamical System Approach to Block Copolymers. *Phys. Rev. A* **1990**, *41*, 6763–6771.
37. Qi, S.; Wang, Z.-G. Kinetics of Phase Transitions in Weakly Segregated Block Copolymers: Pseudostable and Transient States. *Phys. Rev. E* **1997**, *55*, 1682–1697.
38. Ren, S. R.; Hamley, I. W. Cell Dynamics Simulations of Microphase Separation in Block Copolymers. *Macromolecules* **2001**, *34*, 116–126.
39. Pinna, M.; Guo, X.; Zvelindovsky, A. V. Block Copolymer Nanoshells. *Polymer* **2008**, *49*, 2797–2800.
40. Pinna, M.; Guo, X.; Zvelindovsky, A. V. Block Copolymer Nanocontainers. *ACS Nano* **2010**, *4*, 2845–2855.
41. Leibler, L. Theory of Microphase Separation in Block Copolymers. *Macromolecules* **1980**, *13*, 1602–1617.
42. Fredrickson, G. H. Surface Ordering Phenomena in Block Copolymer Melts. *Macromolecules* **1987**, *20*, 2535–2542.
43. Mayes, A. M.; Olvera de la Cruz, M.; McMullen, W. E. Asymptotic Properties of Higher-Order Vertex Functions for Block Copolymer Melts. *Macromolecules* **1993**, *26*, 4050–4051.
44. Owens, J. N.; Gancarz, I. S.; Koberstein, J. T.; Russell, T. P. Investigation of the Microphase Separation Transition in Low-Molecular-Weight Diblock Copolymers. *Macromolecules* **1989**, *22*, 3380–3387.
45. Matsen, M. W.; Schick, M. Stable and Unstable Phases of a Diblock Copolymer Melt. *Phys. Rev. Lett.* **1994**, *72*, 2660–2663.
46. Vigild, M. E.; Almdal, K.; Mortensen, K.; Hamley, I. W.; Fairclough, J. P. A.; Ryan, A. J. Transformations to and from the Gyroid Phase in a Diblock Copolymer. *Macromolecules* **1998**, *31*, 5702–5716.
47. Thomas, E. L.; Refener, J. R.; Bellare, J. A Menagerie of Interface Structures in Copolymer Systems. *J. Phys. Colloques* **1990**, *51*, C7-363–C7-374.
48. Ma, M.; Thomas, E. L.; Rutledge, G. C.; Yu, B.; Li, B.; Jin, Q.; Ding, D.; Shi, A.-C. Gyroid-Forming Diblock Copolymers Confined in Cylindrical Geometry: A Case of Extreme Makeover for Domain Morphology. *Macromolecules* **2010**, *43*, 3061–3071.
49. Ma, M.; Titievsky, K.; Thomas, E. L.; Rutledge, G. C. Continuous Concentric Lamellar Block Copolymer Nanofibers with Long Range Order. *Nano Lett.* **2009**, *9*, 1678–1683.
50. Van Krevelen, D. W. *Properties of Polymers*; Elsevier: Amsterdam, 1990.
51. Vigild, M. E.; Almdal, K.; Mortensen, K.; Hamley, I. W.; Fairclough, J. P. A.; Ryan, A. J. Determination of Interfacial Tensions, Contact Angles, and Dispersion Forces in Surfaces by Assuming Additivity of Intermolecular Interactions in Surfaces. *J. Phys. Chem.* **1962**, *66*, 382.